

Failure characteristics of columns intersected by slabs with different compressive strengths

Seung-Ho Choi¹, Jin-Ha Hwang¹, Sun-Jin Han¹, Hyun Kang², Jae-Yeon Lee³ and Kang Su Kim^{*1}

¹Department of Architectural Engineering, University of Seoul, 163 Siripdaero, Dongdaemun-gu, Seoul, 02504, Korea

²Fire Research Institute, Korea Institute of Civil Engineering & Building Technology (KICT), 64, Mado-ro 182beon-gil, Mado-myeon, Hwaseong-si, Gyeonggi-do 18544, Korea

³Division of Architectural Engineering, Mockwon University, 88 Doanbuk-ro, Seo-gu, Daejeon 35349, Korea

(Received September 18, 2019, Revised February 19, 2020, Accepted February 20, 2020)

Abstract. The objective of this study was to determine the effective compressive strength of a column-slab connection with different compressive strengths between the column and slab concrete. A total of eight column specimens were fabricated, among which four specimens were restrained by slabs while the others did not have any slab, and the test results were compared with current design codes. According to ACI 318, the compressive strength of a column can be used as the effective compressive strength of the column-slab connection in design when the strength ratio of column concrete to slab concrete is less than 1.4. Even in this case, however, this study showed that the effective compressive strength decreased. The specimen with its slab-column connection zone reinforced by steel fibers showed an increased effective compressive strength compared to that of the specimen without the reinforcement, and the interior column specimens restrained with slabs reached the compressive strength of the column.

Keywords: effective compressive strength; joint; reinforced concrete; different concrete strength; failure characteristic; high strength concrete

1. Introduction

Along with the advancement of concrete mixing technology, the use of high-strength concrete (HSC) with over 50 MPa is increasing (Al-Karmal 2019a). It is mainly used on column members to which compressive stress is applied (Urban and Goldyn 2015, Nematzadeh and Fallah-Valukoolae 2017, Bouzid and Kassoul 2018, Bauchkar and Chore 2018, Al-Karmal 2019b). Even though HSC is used on columns, normal-strength concrete (NSC) is often used on slabs due to economic reasons (Choi *et al.* 2018, Gamble and Klinar 1991, Lee and Mendis 2004, Shu and Hawkins 1992). Thus, a difference in compressive strength between the column and slab concrete may lead to decrease in the load transfer performance of the column. To thoroughly consider this issue, the current design codes propose the following three detailed provisions.

1) Puddling method:

According to ACI 318 (2014) the HSC poured in columns should be expanded to at least, or over, 600 mm (500 mm in CSA A23.3 (2014)) in the slab area. This method requires high diligence and proper coordination of construction work, degrading constructability (Urban and Goldyn 2015, Lee and Mendis 2004).

2) Reinforcement of lateral and longitudinal rebars:

Design strength of a column through a floor system shall be calculated using the lower value of concrete strength with vertical dowels and spirals as required to

achieve adequate strength. However, this method is less popular because of not only the lack of design procedures (ACI 318, CSA A23.3) but also a construction problem. In addition, according to Kayani (1992) and Portella (2002), the additional lateral or longitudinal steel rebar placed in the column-slab connection zone did not significantly improve the axial strength.

3) Effective compressive strength (f'_{ce}):

This method applies an effective compressive strength higher than that of the slab concrete but smaller than that of the column concrete to the design. According to ACI 318 (2014), if the compressive strength of the column (f'_{cc}) exceeds 1.4 times the compressive strength of the slab (f'_{cj}), the compressive strength of the slab concrete should be used on corner and edge columns (i.e., $f'_{ce}=f'_{cj}$), and that 75% of the compressive strength of the column concrete and 35% of that of the slab concrete are added together to calculate the effective compressive strength (i.e., $f'_{ce} = 0.75f'_{cc} + 0.35f'_{cj}$). If the compressive concrete of the column (f'_{cc}) is higher than that of the slab (f'_{cj}), CSA A23.3 (2014) uses the compressive strength of the slab as the effective compressive strength in the corner column (i.e., $f'_{ce} = f'_{cj}$). Edge columns use an effective compressive strength 1.4 times the compressive strength of the slab (i.e., $f'_{ce} = 1.4f'_{cj} \leq f'_{cc}$), whereas the interior columns use the addition of the 25% of the compressive strength of column concrete and 105% of that of slab concrete as the effective compressive strength (i.e., $f'_{ce} = 0.25f'_{cc} + 1.05f'_{cj} \leq f'_{cc}$). According to the Ospina and Alexander (1998), when the ratio of column to slab concrete strength exceeds approximately 2.5, the confinement by slab can be

*Corresponding author, Professor
E-mail: kangkim@uos.ac.kr

insufficient to exert the effective compressive strength presented in ACI 318. Therefore, the effective compressive strength in ACI 318 can only be used with a strength ratio of 2.5 or less.

Experimental studies on the effective compressive strength have been conducted by many researchers. (Bianchini *et al.* 1960, Gamble and Klinar 1991, McHarg *et al.* 2000, Ospina and Alexander 1998, Shah *et al.* 2005, Shu and Hawkins 1992, Urban and Gołdyn 2015, Shin *et al.* 2016) Based on these test results, some researchers (Gamble and Klinar 1991, Ospina and Alexander 1998, Shu and Hawkins 1992) proposed equations for calculating the effective compressive strength. However, there are still a lack of the test results especially for the interior columns.

In this study, axial compression test was conducted on sandwich column specimens that represent corner and edge columns and interior column specimens, four sides of which were restrained by slabs. The test results were then compared with the existing design codes. In addition, the measured strain distribution of the sandwich and interior column specimens were compared and analyzed.

2. Experimental investigation

2.1 Test variables and specimen details

Fig. 1 and Table 1 show the details of the test specimens. The compressive strengths of the columns were expressed as the average strengths of the upper and lower columns because they had the same mixture design. The control specimen C1 in Fig. 1(a) had no intersecting weak joint layer, and its compressive strength was 51.2 MPa. Specimens C2 and C3 in Fig. 1(b) are sandwich columns, which are simulations of the concrete casting with different compressive strength between the upper and lower columns and slabs. To follow the construction process in real buildings, these specimens were made by pouring concrete in the following order: lower column, joint, and upper column. The longitudinal reinforcement consisted of 4-D13 deformed bars in all columns, and D6 hoop reinforcement as shown in Fig. 1. The yield and ultimate strength of each reinforcement were as shown in Table 2. The compressive strength ratio of the column and the joint concrete (f'_{cc}/f'_{cj}) in the C2 specimen was 1.35, at which ACI 318 (2014)

allow the compressive strength of the column concrete to be used as the effective compressive strength. f'_{cc}/f'_{cj} of C3 specimen was 1.44, and at that point, the compressive strength of the column concrete exceeded 1.4 times, the compressive strength of the joint; therefore, the reduction of concrete compressive strength needed to be considered. All the details of the S1 specimen in Fig. 1(c) were identical to those of the C3 specimen, except for the reinforcement of the joint with steel fiber. In this study, the bundled type hooked-end steel fibers were used, and the length and diameter of steel fibers were 30 mm and 0.50 mm, respectively. The tensile strength, density, and the volume fraction of the steel fiber were 1,100 MPa, 7.85 kg/m³, and 1.5 %, respectively.

Specimens I1~I4 in Fig. 2 are the interior columns whose four sides were restrained by slab. The length of the slab is 1,200 mm, and D10 deformed bars were used for the flexural reinforcement for the slab in both directions 120 mm apart. Specimen I1 was a control specimen, and while its column and slab should have been made as a unit, due to the production conditions, both the column and the slab could not be cast in concrete at the same time. Therefore, they were cast in sequence. Nevertheless, the compressive strength of the column and slab concrete of specimen I1 were almost identical at 51.2 and 49.8 MPa (i.e., $f'_{cc}/f'_{cj} = 1.027$), respectively. The concrete compressive strength of specimens I2 and I3 were identical to C2 and C3 specimen, respectively. The concrete compressive strength of the column and slab of specimen I4 were 49.8 MPa and 35.5 MPa, respectively.

2.2 Test setup and instrumentation

Fig. 3 shows the test setup for the specimens in C series, S1, and I series. The axial compression test was performed using a 5,000 kN capacity universal testing machine, and to measure the axial displacement of the upper, lower columns and slab, linear variable differential transformers (LVDTs) were installed. Also, to measure the horizontal strain near the interface of the slab-column, three concrete embedded gages were installed 50 mm apart from the slab-column interface, as shown in Figs. 1 and 2.

The upper and lower parts of the column were restrained by metal shoes to prevent local damage by stress concentration. Existing studies (Gamble and Klinar 1991,

Table 1 Summary of dimensions and material properties of test specimens

	type	c (mm)	h (mm)	f'_{cc} (MPa)	E_{cc} (MPa)	f'_{cj} (MPa)	E_{cj} (MPa)	A_s (mm ²)	f'_{cc}/f'_{cj}	Note
C1	isolate	200	100	51.2	45,582	51.2	45,582	506.8	1.00	Control (isolate)
C2	sandwich	200	100	47.8	48,540	35.5	40,868	506.8	1.35	-
C3	sandwich	200	100	51.2	45,582	35.5	40,868	506.8	1.44	-
S1	sandwich	200	100	51.2	45,582	35.5	40,868	506.8	1.44	1.5% steel fiber
I1	interior	200	100	51.2	45,582	49.8	46,852	506.8	1.03	Control (interior)
I2	interior	200	100	47.8	48,540	35.5	40,868	506.8	1.35	-
I3	interior	200	100	51.2	45,582	35.5	40,868	506.8	1.44	-
I4	interior	200	100	49.8	46,852	35.5	40,868	506.8	1.40	-

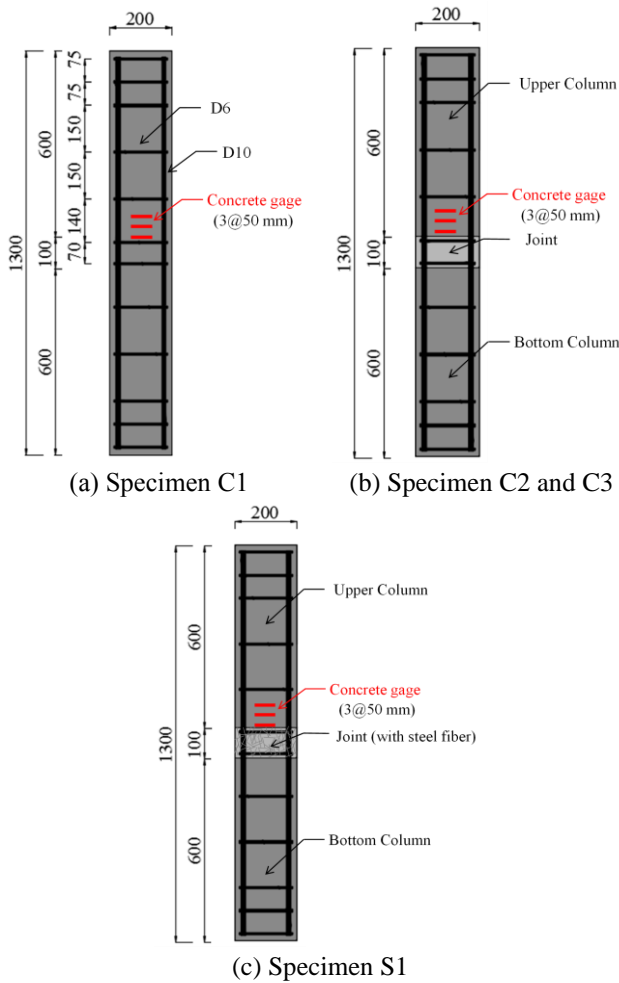


Fig. 1 Specimen details (C series and S1) (Unit: mm)

Bianchini *et al.* 1960, Ospina and Alexnader 1998, McHarg *et al.* 2000) conducted their interior column test under the free edge condition by not having the slab restraining force.

However, the interior columns in real building are restrained by a slab that has very large axial stiffness. Thus, such an interior column test on the slab with free edge condition would underestimate the restraining effect of the slab. Therefore, in this study, the slab was restrained with an exterior frame as shown in Fig. 4 in order to reflect in the restraining effect by slab during the tests on specimens I1~I4. The flexural reinforcement placed in the slab was extended outside the member, and the ending was processed with spiral shape so as to assemble it with nuts.

3. Experimental results

3.1 Compressive behavior of test specimens

Fig. 5 shows the applied load – axial strain curves of each specimen. The axial strain is the average strain calculated by dividing the all axial displacement between the endings of the upper and lower columns by the length of the total column. The current design codes (ACI 318, 2014; CSA A23.3, 2014) present the nominal axial strength (P_0) of the concrete without eccentricity as follows:

Table 2 Yield and ultimate strengths of reinforcements

	f_y (MPa)	f_u (MPa)
D6	435.6	497.3
D10	499.4	590.1
D13	419.2	621.0

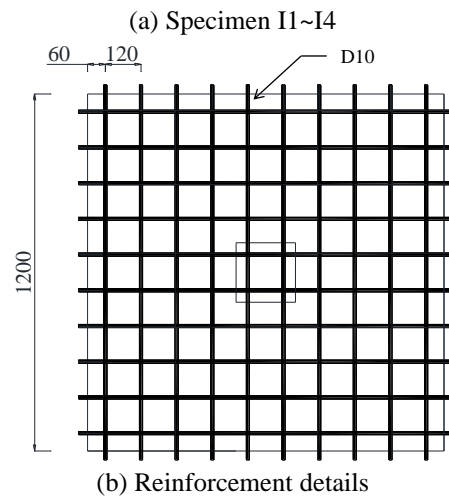
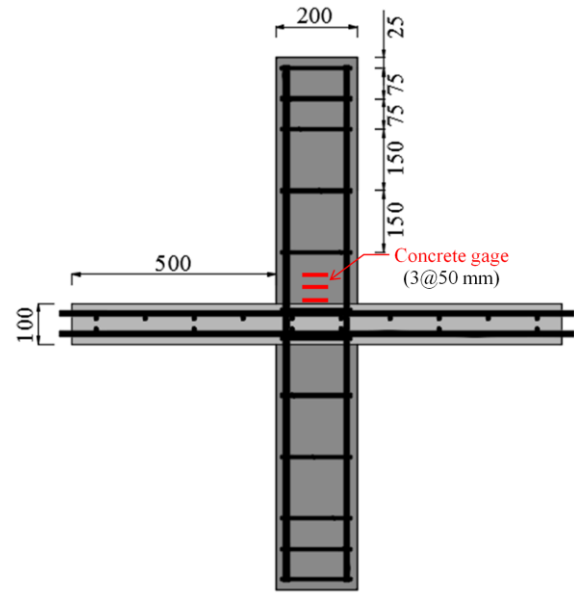


Fig. 2 Specimen details (I series) (Unit: mm)

$$P_0 = \alpha f'_c (A_g - A_s) + A_s f_y \quad (1)$$

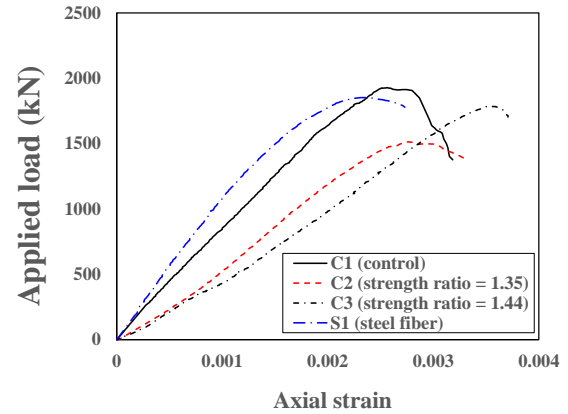
where, α is the stress block parameter that reflects the difference between the strength of the column concrete and cylinder concrete (Shin *et al.* 2016), which is 0.85 in ACI 318 (2014) or $0.85 - 0.0015 f'_c$ in CSA A23.3 (2014), f'_c being concrete compressive strength. A_g and A_s are the sectional area of the column concrete and the longitudinal reinforcement, respectively. f_y represents the yield strength of longitudinal reinforcement. In this study, Eq. (1) and the maximum axial load of the column measured in the test (P_{test}) are used to calculate the effective compressive strength of the specimen ($f'_{ce, test}$) as follows:

Table 3 Maximum load and effective column strength of each specimen

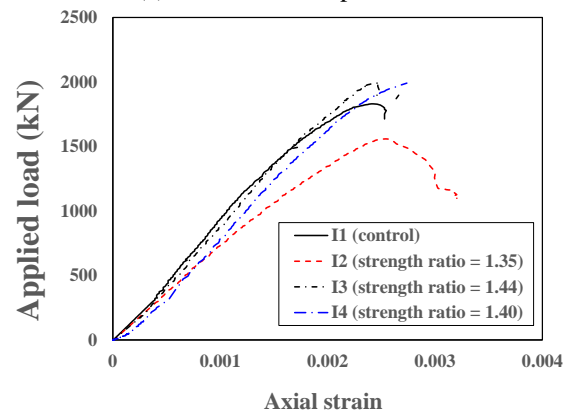
	P_{test} (kN)	$f'_{ce,test}$ (MPa)
C1	1928.0	51.1
C2	1512.6	38.7
C3	1786.7	46.9
S1	1852.5	48.9
I1	1831.0	48.2
I2	1558.7	40.1
I3	1993.7	53.1
I3	1991.0	53.0

and 53.0 MPa, respectively. The concrete compressive strength of I2 and I3 specimens was identical to that of C2 and C3 specimens, respectively, and compared to C2 and C3 specimens, their effective compressive strength increased by 3.6 % and 13.2 %, respectively. The improvement was due to the slab restraining effect. The effective compressive strength (53.1 and 53.0 MPa) were higher than the compressive strength (51.2 and 49.8 MPa) of the column of specimens I3 and I4. It is so because the quality coefficient 0.85 was applied to the calculation of the effective compressive strength of I3 and I4 as shown in Eq. 2. As such, if the restraining force of the slab is high, the effective compressive strength of the column-slab will reach the compressive strength of the column.

Figs. 6 and 7 show the crack patterns at the failure of the specimens in C series, S1, and I series. Specimen C1 showed the most cracks on the upper area of the column whereas specimen C2 showed damage on the joint as well as many cracks on the upper area of the column. Specimen C3 and S1 showed considerable cracks on the upper, joint and lower area of the column. I series specimens exhibited the most cracks on the upper area of the column, and only specimen I1 showed minor cracks on the lower area of the column. The previous test on effective compressive strength of the slab-column connection (Gamble and Klinar 1991, Bianchini *et al.* 1960, Ospina and Alexander 1998, McHarg *et al.* 2000) showed many cracks on the surface of the slab. The I series specimens performed in this study, however, did not show any cracks on the surface or side of the slab. This is because the previous test on interior column specimens used the free edge condition without restraining the slab, whereas the specimens performed in this study restrained the slab by the exterior frame. Fig. 8 shows the strain conditions of the specimens under the free edge condition without gravity loads or restraints. As axial force was applied to the column, the C region of the column was forced to expand in the radial direction by the Poisson effect. This caused the tensile strain on the slab, as indicated by the arrow in area A, and on the extension line of the interface of the column, and the compressive strain (the arrow in area B) by the slab restraining on the column interface. Due to this strain, even though the slab is under the free edge condition, the effective compressive strength of the column increases more than that of the sandwich column. Moreover, the cracks develop on the slab due to the



(a) C1~C3 and S1 specimens



(b) I1~I4 specimens

Fig. 5 Applied load-axial strain responses

tensile strain in area A, the strain by the Poisson effect in area C increases, resulting in the reduction of the restraining force by the slab. However, real buildings have slabs in series, and thus, the stiffness of slab is quite large compared to that in the test specimens. Furthermore, when the compressive force is applied to the column, the lateral strain is restrained by the slabs, and therefore, the slab cracks by the Poisson effect on the column do not occur. Thus, it should be taken into consideration when analyzing the existing test results based on the free edge.

3.2 Comparison with current design codes

Figs. 9 and 10 are comparisons of the results from literature review (Gamble and Klinar 1991, Lee and Mendis 2004, Shu and Hawkins 1992, Bianchini *et al.* 1960, Ospina and Alexander 1998, McHarg *et al.* 2000, Shah *et al.* 2005, Lee *et al.* 2007) on the sandwich, corner and edge columns, including the test results from this study, and the effective compressive strength equation presented in the current design codes. In the previous tests conducted by other researchers (Shu and Hawkins 1992, Ospina and Alexander 1998), the effective compressive strength tended to decrease as the h/c ratio increased. In fact, the authors also reported the same phenomenon in the other research (Choi 2019). Figs. 9 and 10 show that the current design codes estimate the effective compressive strength mostly on the safe side, and the level of safety margin becomes larger when the f'_{cc}/f'_{cj} ratio increases and the h/c ratios decreases. In

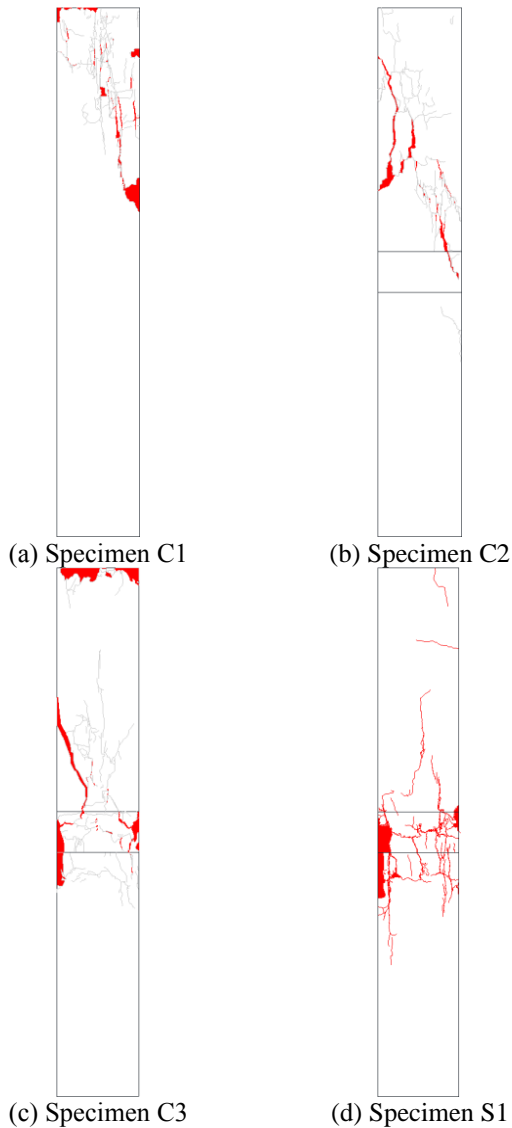


Fig. 6 Crack patterns at compression failure (C series and S1 specimens)

fact, the h/c ratios are less than 1.0 in most buildings, and in this range the f'_{cc}/f'_{cj} ratios are very conservative and the safety margin is quite large.

As shown in Figs. 9 and 10, ACI 318 (2014) and CSA A23.3 (2014) evaluated the test results on the sandwich, corner and edge columns to be safe. The analysis results from ACI 318 (2014) showed that the average (AVG) of the ratio of the test results to the analysis results ($f'_{ce}/f'_{ce, test}$) was 0.687, which was a very conservative result, and the coefficient of variation (COV) was 0.325 with a large deviation of $f'_{ce}/f'_{ce, test}$. The effective compressive strength from CSA A23.3 (2014) also showed the AVG of $f'_{ce}/f'_{ce, test}$ and COV to be 0.633 and 0.277, which were considerably conservative. However, it should be noted that the ACI 318 (2014) provided unsafe analysis results in the case of this study's specimen C2 where the compressive strength ratio of the column concrete to the slab concrete (f'_{cc}/f'_{cj}) was lower than 1.4.

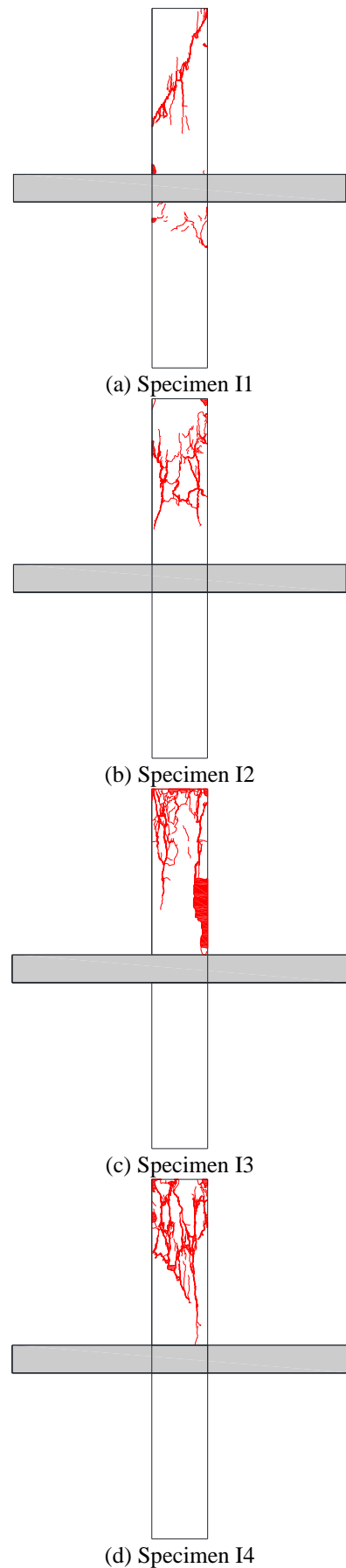


Fig. 7 Crack patterns at compression failure (I series specimens)

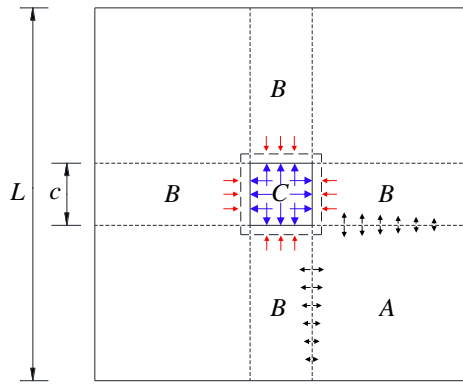
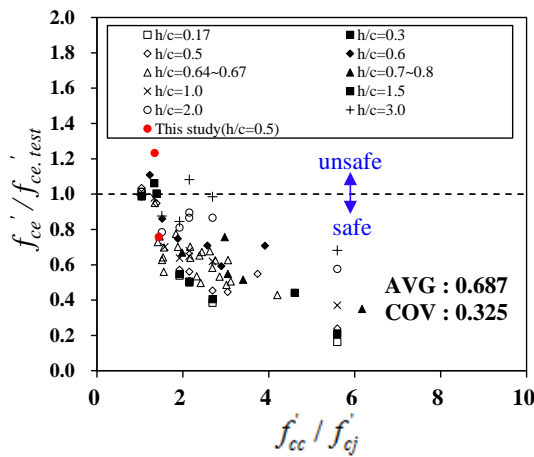
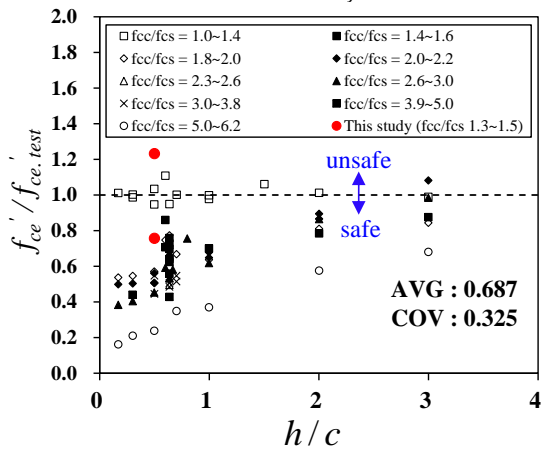


Fig. 8 Strain distribution of interior column specimens at free edge condition



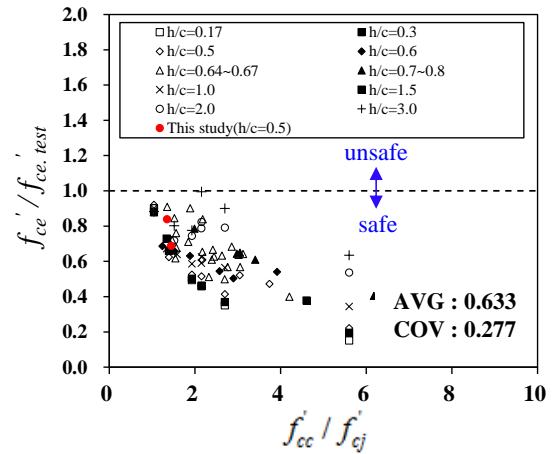
(a) Effect of f'_{cc}/f'_{cj} ratio



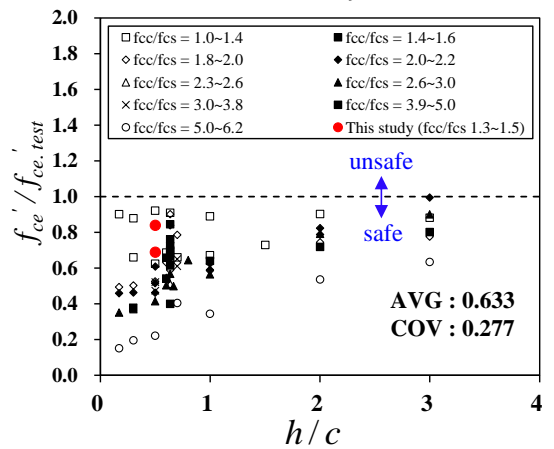
(b) Effect of h/c ratio

Fig. 9 Comparison of test results and ACI 318-14 (C series)

Fig. 11 shows a comparison of the test and analysis results on the interior columns with unloaded slabs. The calculation results based on ACI 318 (2014) shows the AVG at 1.016 and the COV at 0.130, which were in excellent accuracy, compared to the results on the sandwich, corner and edge columns. However, they also recorded unsafe results on several specimens. The calculation results by CSA A23.3 (2014) showed the AVG at 0.707 and the COV at 0.130, and while the accuracy was



(a) Effect of f'_{cc}/f'_{cj} ratio



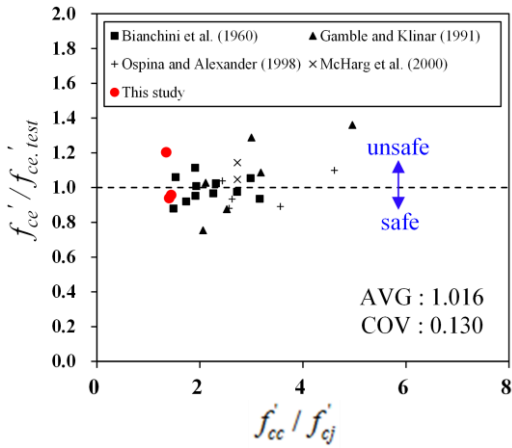
(b) Effect of h/c ratio

Fig. 10 Comparison of test results and CSA A23.3 (C series)

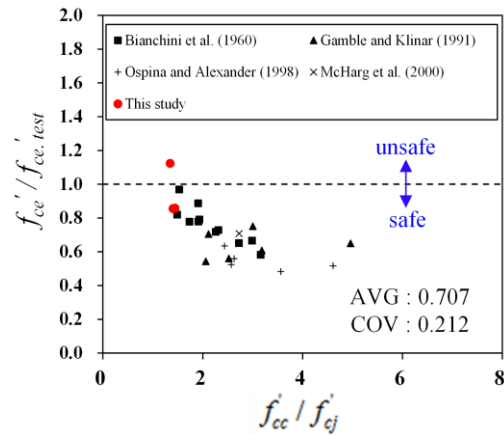
somewhat improved compared to the analysis results on the sandwich, corner and edge columns, these were still very conservative. Since most specimens were made in the free edge condition without any restraint, it is believed that future tests should take into consideration various restraining conditions. It should also be noted that the gravity load applied to the slab, according to the previous studies (Ospina and Alexander 1998, Shah *et al.* 2005), reduces the restraining effect of the slab in the slab-column connecting zone. Therefore, further tests are required on the columns by considering the slab restraining conditions and the gravity load applied to the slab.

3.3 Lateral strain distribution

Fig. 12 showed the measured horizontal strain on the column using the concrete embedded gages near the slab-column interface. Choi *et al.* (2018) pointed out that even without the restraining of the slab onto the column, to satisfy the strain compatibility condition, horizontal tensile stress is applied to the column on the slab-column interface, and horizontal compressive stress is applied to the slab. Due to such horizontal stresses, the compressive strength of the column concrete decreases while the compressive strength



(a) ACI 318-14



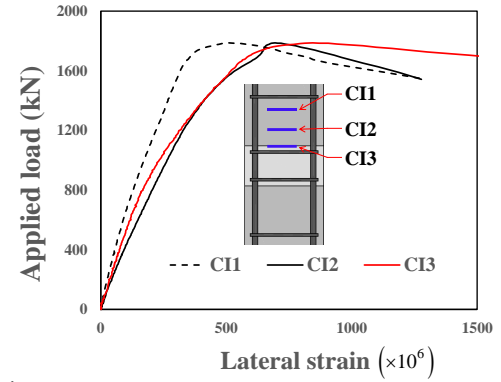
(b) CSA A23.3-14

Fig. 11 Comparison of test results and current design codes (I series)

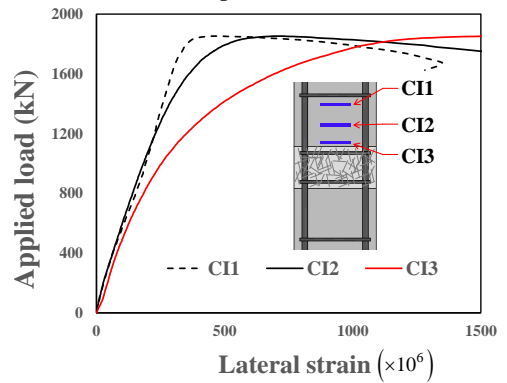
of the slab concrete increases. Specimen C3 in Fig. 12(a) shows that an increase in distance from the joint leads to decrease in the lateral strain. This is believed to be the reason for the higher lateral strain in CI2 and CI3 than in CI1 due to the horizontal stress generated on the slab-column interface, as reported by Choi *et al.* (2018). Such a tendency is identical to that shown in specimen S1 of Fig. 12(b). However, the specimen in I series, with column restrained by the slab, showed a different tendency in the strain distribution. In other words, as shown in Fig. 12(c), the strains measured from CI2 and CI3 are lower than those of CI1. This demonstrated that, compared to the sandwich, corner, and edge columns where the tensile stresses are produced in the column near the slab-column interface, in the case of interior columns, the horizontal strains in the column near the slab-column interface are restrained by the slab. Thus, the joint of the interior column is under the three-axis compression condition due to the restraining of the slab, resulting in the increase of the effective compressive strength.

4. Conclusions

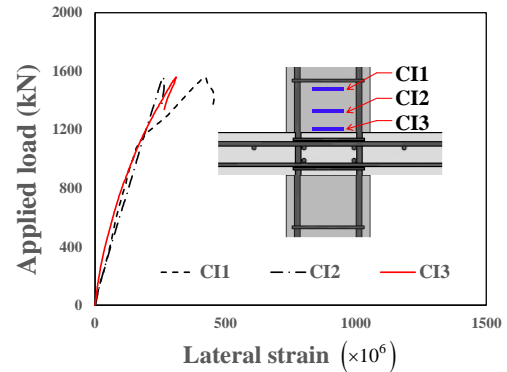
The objective of this study was to determine the effective compressive strength of the column-slab connection with different compressive strengths between



(a) Specimen C3



(b) Specimen S1



(c) Specimen I2

Fig. 12 Measured lateral strain distribution

the column and slab concrete, and the test results were compared to the existing design codes. Also, a detailed comparison and analysis of the strain measured from the strain gages were carried out to verify by experiments the restraining effect of the slab on the interior column. From this study, the following conclusions are derived.

1) Effective compressive strengths of specimens C2 and C3 whose strength ratios of the column to the slab concrete are 1.35 and 1.44, respectively, were lower than those of the column concrete by about 20.0 % and 8.4%, respectively. The effective compressive strength of the specimen S1 with steel fibers was increased by 4.2%. In cases of the specimen I2 and I3, the effective compressive strengths increased 3.6 and 13.2%, respectively, due to restraints of the exterior frames.

2) According to the test results on the sandwich columns, despite the strength ratio of the column to the slab

concrete (f'_{cc}/f'_{cj}) being less than 1.4, the strength of the column concrete may decrease. Therefore, it is reasonable to reduce the critical strength ratio ($(f'_{cc}/f'_{cj})_{critical}$) of the column concrete to the slab concrete proposed by ACI 318 (2014) to 1.0.

3) To determine the effect of steel fiber on the effective compressive strength of the column quantitatively, additional experimental and analytical research is necessary.

4) Compared to the sandwich column specimen C3 where the tensile stresses are produced in the column near the slab-column interface, in the case of interior column specimen I2, the horizontal strains in the column near the slab-column interface are restrained by the slab.

5) In real buildings, the slab-column connection in the interior column is under three-axis compression status due to the restraining of the slab, and thus, this study introduced the restraining force to the slab using the exterior frame. The result showed that the effective compressive strength of the slab-column was identical to the compressive strength of the column.

6) However, the restraining conditions of the slab depends on the effect of gravity load applied to the slab, and therefore, further research is required.

Acknowledgments

This research was supported by the National Research Foundation of Korea (NRF) (2017R1D1A3B03028005) for Jae-Yeon Lee. Also, this research was supported by the 2019 Research Fund of the University of Seoul for Kang Su Kim.

References

- ACI 228.2R-13 (2013), "Nondestructive test methods for evaluation of concrete in structures", *American Concrete Institute Report*, Farmington Hills, U.S.A.
- ACI Committee 318 (2014), Building Code Requirements for Structural Concrete and Commentary, American Concrete Institute.
- Al-Kamal, M.K. (2019), "Nominal Flexural Strengths of High-Strength Concrete Beams", *Adv. Concr. Constr.*, **7**(1), 1-9. <https://doi.org/10.12989/acc.2019.7.1.001>.
- Al-Kamal, M.K. (2019), "Nominal Axial and Flexural Strengths of High-Strength Concrete Columns", *Comput. Concrete*, **24**(1), 85-94. <https://doi.org/10.12989/cac.2019.24.1.085>.
- Bauchkar, S.D., and Chore, H.S. (2018), "Experimental study on rheology, strength and durability properties of high strength self-compacting concrete", *Comput. Concrete*, **22**(2), 183-196. <https://doi.org/10.12989/cac.2018.22.2.183>.
- Bouزيد, H., and Kassoul, A. (2018), "Curvature Ductility Prediction of High Strength Concrete Beams", *Struct. Eng. Mech.*, **66**(2), 195-201. <https://doi.org/10.12989/sem.2018.66.2.195>.
- Bianchini, A.C., Woods, R.E., and Kesler, C.E. (1960), "Effect of Floor Concrete Strength on Column Strength", *ACI J. Proc.*, **56**(5), 1149-1170. <https://doi.org/10.14359/8135>.
- CSA Committee A23.3 (2014), Canadian Standards Association Design of Concrete Structure, Canadian Standards Association.
- Choi, H.K., Bae, B.I., and Choi, C.S. (2015), "Mechanical Characteristics of Ultra High Strength Concrete with Steel Fiber under Uniaxial Compressive Stress", *J. Korea Concr. Inst.* **27**(5), 521-530. <https://doi.org/10.4334/JKCI.2015.27.5.521>.
- Choi, S.H. (2019), "Effective Compressive Strengths of High Strength Concrete Columns Intersected by Normal Strength Concrete Slab", Ph.D. Dissertation, Department of Architectural Engineering, University of Seoul.
- Choi, S.H., Lee, D.H., Hwang, J.H., Oh, J.Y., Kim, K.S. and Kim, S.H. (2018), "Effective Compressive Strength of Corner and Exterior Concrete Columns Intersected by Slabs with Different Compressive Strengths", *Arch. Civ. Mech. Eng.* **18**(3), 731-741. <https://doi.org/10.1016/j.acme.2017.11.001>.
- Gamble, W.L., and Klinar, J.D. (1991), "Tests of High-Strength Concrete Columns with Intervening Floor Slabs", *ASCE J. Struct. Eng.* **117**(5), 1462-1476. [https://doi.org/10.1061/\(ASCE\)0733-9445\(1991\)117:5\(1462\)](https://doi.org/10.1061/(ASCE)0733-9445(1991)117:5(1462)).
- Hwang, J.H., Lee, D.H., Kim, K.S., Ju, H.J., and Seo, S.Y. (2013), "Evaluation of Shear Performance of Steel Fiber Reinforced Concrete Beams using a Modified Smeared-Truss Model", *Mag. Concrete Res.*, **64**(5), 283-296. <https://doi.org/10.1680/macr.12.00009>.
- Karl, K.W., Lee, D.H., Hwang, J.H., Kim, K.S., and Choi, I.S. (2011), "Revision on Material Strength of Steel Fiber-Reinforced Concrete", *Int. J. Concr. Struct. M.*, **5**(2), 87-96. <https://doi.org/10.4334/IJCSM.2011.5.2.87>.
- Kayani, M.K. (1992), "Load Transfer from High-Strength Concrete Columns through Lower Strength Concrete Slabs", Ph.D. Dissertation, Department of Civil Engineering, University of Illinois, Urbana-Champaign, III.
- Lee, S.C., and Mendis, P. (2004), "Behavior of High-Strength Concrete Corner Columns Intersected by Weaker Slabs with Different Thicknesses", *ACI Struct. J.*, **101**(1), 11-18. <https://doi.org/10.14359/12993>.
- Lee, J.H., Yang, J.M., Lee, S.H., and Yoon, Y.S. (2007), "Improved Transmission of UHSC Column Loads by Puddling of Fiber Reinforced UHSC", *J. Korea Concr. Inst.*, **19**(2), 209-216. <https://doi.org/10.4334/JKCI.2007.19.2.209>.
- Nematzadeh, M., and Fallah-Valukolaee, S. (2017), "Effectiveness of fibers and binders in high-strength concrete under chemical corrosion", *Struct. Eng. Mech.*, **64**(2), 243-257. <https://doi.org/10.12989/sem.2017.64.2.243>.
- McHarg, P.J., Cook, W.D., Mitchell, D., and Yoon, Y.S. (2000), "Improved Transmission of High-Strength Concrete Column Loads through Normal Strength Concrete Slabs", *ACI Struct. J.*, **97**(1), 149-157. <https://doi.org/10.14359/845>.
- Ospina, C.E., and Alexander, S.D.B. (1998), "Transmission of Interior Concrete Column Loads Through Floors", *ASCE J. Struct. Eng.*, **124**(6), 602-610. [https://doi.org/10.1061/\(ASCE\)0733-9445\(1998\)124:6\(602\)](https://doi.org/10.1061/(ASCE)0733-9445(1998)124:6(602)).
- Portella, G. (2002), "Transmission of High-Strength Concrete Column Loads Through Normal-Strength Concrete Slabs", M.Sc Dissertation, Department of Civil Engineering, University of Melbourne, Victoria, Australia.
- Shah, A.A., Dietz, J., Tue, N.V., and Koenig, G. (2005), "Experimental Investigation of Column-Slab Joints", *ACI Struct. J.*, **102**(1), 103-113. <https://doi.org/10.14359/13535>.
- Shu, C.C., and Hawkins, N.M. (1992), "Behavior of Columns Continuous Through Concrete Floors", *ACI Struct. J.*, **89**(4), 405-414. <https://doi.org/10.14359/3023>.
- Urban, T.S., and Goldyn, M.M. (2015), "Behaviour of Eccentrically Loaded High-Strength Concrete Columns Intersected by Lower-Strength Concrete Slabs", *Struct. Concr.*, **16**(4), 480-495. <https://doi.org/10.1002/suco.201400114>.